

Representation and Verification of Offline Signatures with Dictionary Learning and Parsimonious Coding

Elias N. Zois^a, Dimitrios Tsourounis^b, Ilias Theodorakopoulos^b, Anastasios Kesidis^c, and George Economou^b

^aLaboratory of Telecommunications and Signal Processing, Electrical and Electronic Engineering Department, University of West Attica, Campus I, Egaleo, 12243, Greece.
email: ezois@teiath.gr

^bElectronics Laboratory, Physics Department, University of Patras, Patras 26500, Greece.
email: {dtsourounis, iltheodorako, economou}@upatras.gr

^cGeospatial Technology Research Laboratory, Department of Surveying and GeoInformatic Engineering University of West Attica, Egaleo, 12243, Greece.
email: akesidis@teiath.gr

Abstract—In this work, a method for offline signature verification is presented that harnesses the power of sparse representation in order to deliver state-of-the-art verification performance in several signature datasets like CEDAR, MCYT-75, GPDS and UTSIG. Beyond the accuracy improvements, several major parameters associated with sparse representation; such as selected formulation, dictionary size, sparsity level and positivity priors are investigated. Besides, it is evinced that 2nd order statistics can be a powerful pooling function for the formation of the global signature descriptor. Also, a thorough evaluation of the effects of preprocessing is introduced by an automated algorithm in order to select the optimum thinning level. Finally, a segmentation strategy which employs a special form of spatial pyramid tailored to the problem of sparse representation is presented along with the enhancing of the produced descriptor on meaningful areas of the signature as emerged from the BRISK key-point detection mechanism. The obtained state-of-the-art results on the most challenging signature datasets provide a strong indication towards the benefits of learned features, even in WD scenarios with only a few available reference samples.

Index Terms—Off-line Signature Verification, Dictionary Learning, Sparse Coding, Spatial Pyramid, Feature Pooling, Image Preprocessing

I. INTRODUCTION

One of the most acceptable and long-standing modus to declare and verify a person's identity or acknowledge of his/hers consent in a wide variety of cases is the handwritten signature, which is a behavioral biometric trait. Its production includes a personal motoric pattern shaped from a potential mixture of letters and/or an intricate flourish [1, 2] and it is considered also to be the combined result of a person's specific motoric procedure and his/hers taught scripting customs.

Signatures are depicted by their trace, usually onto a sheet of paper or an electronic device and is a process which conveys information related not only to the imprinting of the personal details of the signatory, but also to his/her writing system and psychophysical state [3]. Ongoing research regarding the development of Automated Signature Verification Systems (ASV's/SV's) indicate clearly that this topic still is an active, open and important research field [4-7].

The acquisition methods of the handwritten Signature Verification systems (SV's) fall within two major categories [8]: The first one is the online method, in which the trace is captured in real time using specialized acquisition devices like tablets or smart phones [5]. The second one is the offline or static method, in which the generated signature trace is depicted in a form of a still image, as a result of a scanning procedure. Both types of systems are responsible for carrying out the task of authenticating an individual by means of his/hers signature with the use of computer vision and pattern recognition (CVPR) techniques. Their purpose is twofold: a) to potentially support forensic document examiners (FDE's) in order to provide an informed opinion concerning the genuineness or not of a sample in question [9] as well as b) to provide a non-invasive, user-friendly and secure interface for security oriented e-society applications. Offline signature verification systems depend solely on static images and have been reported to exhibit inferior performance compared to on-line systems [10, 11] but their use may be the only option, especially in forensic applications [12, 13].

The purpose of a SV system is to recognize a signature in question as genuine or forgery, i.e. to verify the writer's genuine signatures and reject the forgery ones. There are four main types of forgery signatures [14]: a) Random: defined as genuine signatures of a writer different from the claimed author, b) Simple/Casual/Zero Effort: defined as signature samples that are formed by an imitator who owns the name of

the genuine writer or samples that are formed by someone who knows the original signatures but his efforts are without practicing, c) Simulated/Skilled: samples that are formed by an experienced imitator or a calligrapher after practicing unrestricted number of times, d) Disguised: samples that actually are not a forgery, but instead they are the outcome of an effort of a genuine author to imitate his/her own signature in such a way that he/she can deny it at a later time.

The basic stages of a SV system include tasks like: a) preprocessing, in which the original images are subjected to enhancement in order to remove artifacts which distort its content, b) feature extraction, in which any input signature image is transformed into a vector of numerical values under an underlying hypothesis regarding its content and c) decision, in which a classifier is used in order to decide the claimed authenticity of the sample in question. The outcome of the classifier is usually expressed by means of either a binary decision or/and an underlying score which may be regarded as a probability or confidence measure.

Conceivably, the most influential step in the design of a SV system is the feature extraction stage, which can be defined as the process that maps any given signature image into a multidimensional vector. Signatures are carriers of intrinsic ambiguity since they are different even when they are formed by the same person [15]. Thus, a signature's descriptor should be designed in such a way as to provide both enough discrimination- in order to distinguish genuine from forgeries- and robustness to the significant intra-class variability. Feature extraction methods can be divided into two major categories [4]: a) handcrafted features which aim at pre-determined characteristics of the image; examples of this branch include methods with global-local and/or grid-texture oriented features [16-18] and b) features learned directly from images, where Deep Learning (DL) [19], [4], [20], Bag of Visual Words (BoW) [21-23] or Histogram of Templates (HOT) [24] are some of the most representative techniques.

Learning features from images could potentially have significant advantages, since such techniques -in general- can discover specialized spatial associations that are inherent into the signature images. Among the most powerful classes of such methods is Sparse Representation (SR). Sparse Representation aims to provide a parsimonious representation of a signal by means of a linear combination of only a few atoms, which are members of an overcomplete set or dictionary-lexicon. They have been the object of scientific interest for quite a long time [25, 26] and have been proved to be extremely useful in computer vision and pattern recognition applications.

Signature Verification systems are categorized according to the way that they construct the verification model. More specifically, if one individual model is trained for each writer in order to recognize the genuine signatures of writer from the forgeries, it is characterized as a Writer-Dependent (WD) system. The WD systems are more commonly used and the writer's WD model is constructed utilizing a small number of samples from each writer. On the contrary, if a unique signature verification model is used for all the writers, it is

referred as the Writer-Independent (WI) approach. In this case, a global model is designed and most of the time, the WI system is trained and tested with a different subset of users. The WI systems are introduced in order to overcome the problem of limited availability of reference samples from each individual, suffering though from the need of diverse examples in order to construct a realistic global model. This work addresses the first type of signature verification (WD) by employing a unique model for each participating writer with the use of some genuine reference samples and some genuine samples from other writers as representatives of the positive and negative class respectively.

In addition, this work presents a method for offline signature verification that harnesses the power of SR in order to deliver state-of-the-art verification performance with the use of few genuine reference samples. The current paper introduces several advancements in the line of work that was initiated with two recently published papers investigating the potential of SR [16] and Archetypal Analysis (AA) [17] on the offline SV task. Beyond the accuracy improvements and the high-end performance achieved in several popular signature datasets, this work has a significant contribution towards the following directions:

- We thoroughly investigate the impact of all the major parameters associated with SR, such as selected formulation (greedy approximation or convex relaxation), dictionary size, sparsity level etc. We also evaluate the effect to the overall performance of imposing additional priors into the corresponding optimization problems.
- We innovatively address several aspects of local feature pooling. A segmentation strategy which employs a special form of spatial pyramid (SP) tailored to the problem of SV is presented, and a number of alternative pooling functions are evaluated. Also, we demonstrate the efficiency of 2nd order statistics as a powerful pooling function for the formation of the global signature descriptor.
- We apply a standard mechanism for enhancing the verification efficiency of the produced descriptor on meaningful areas of the signature, by means of the key-point detection mechanism of BRISK descriptors.
- We perform a thorough evaluation of the effects of preprocessing, especially thinning and introduce an automated algorithm to select the optimum thinning level in order to derive a signature's trace on the image plane.

The paper is organized as follows: Section 2 provides a short literature review and summarizes the proposed approach. Section 3 provides some necessary elements on theory and formulation of sparse representation along. Section 4 discusses details of the signature preprocessing steps along with the feature formation process and Section 5 describes the utilized databases along with the evaluation protocol. Section 6 displays the corresponding experimental results. Finally, conclusions are drawn in Section 7.

II. LITERATURE REVIEW AND SUMMARY OF THE METHOD

A. Related Work

Writer dependent methodologies are characterized by the fact that a dedicated classifier is created for each person under consideration [27], providing the advantage of extra security since no templates are stored [28]. Examples of classifiers used in offline WD systems include, among others, artificially immune recognition systems [29], [30], hidden Markov models [31], [32], [33] neural networks [34], distance classifier [33], [35], SVMs [33], [36], [37] and deep learning methods [38]. There are two main shortcomings regarding the use of WD-oriented systems [28], [39]: First, the necessity of learning a unique model each time a new writer is inserted in the system [40] and second the relative large number of genuine samples that are required to build a reliable model by means of significant class statistics estimation errors. For example, with the use of few positive negative class examples we are at the limit (maybe a bit beyond) of the ability of generalization of a classifier such as a support vector machine (SVM) which is not designed for so few data. Despite these issues, WD systems are performing quite well, even when only a few reference samples are available. Additionally, in order to overcome such problems, a potential solution could emerge from synthetic signature samples [41], [42]. Recently mixed implementations have been also presented [28], [4] with notable results.

All things considered, the SV's can be also distinguished according to the way that the signature is modeled and projected into the feature space. A significant number of handcrafted feature extraction methods for offline signature verification rely on the evaluation of global and/or local signature descriptors as well as on grid-texture oriented features. With respect to the above family of feature descriptors, a diversity of feature extraction methods for offline SV has been proposed. Examples include Granulometric Size Distributions [43], Extended Shadow Code (ESC) and Directional Probabilistic Density Functions (DPDF) [27, 28], variations of Local Binary Patterns (LBP) [24, 36, 44], Histogram of Oriented Gradients (HOG) [19, 45], surroundness [40], curvelet transform [46], Directional Code Co-occurrence Matrix (DCCM) [47] or Co-occurrence Matrix [48], Interval Symbolic Representation [49], Speeded Up Robust Features (SURF) [13, 50] partially ordered sets [18, 51], KAZE or local correlated features [21-23], Slant [52], Discrete Radon Transform (DRT) [19, 31, 53], Modified Direction Feature (MDF) [54], Optical Flow [37, 55], Graphometrics [56], Scale Invariant Feature Transform (SIFT) [57], Morphology [58], and Ring-peripheral features [59].

On the other side methods have been proposed that rely on learning features from the raw image data. Some efforts include the use of Restricted Boltzmann Machines (RBMs) in [60] and Convolutional Neural Networks (CNNs) [61], [62]. Soleimani et al. in [19] proposed the use of Deep Neural Networks for Multitask Metric Learning by employing a distance metric between pairs of signatures in which Local Binary Patterns were used as an intermediate feature vector.

Rantzsch et al. [63] presented an approach named Signature Embedding which is based on deep metric learning. Specifically they compared triplets of two genuine and one forged signature, in order for their system to learn to embed signatures into a high-dimensional space. Following, they proposed a Euclidean distance metric as a means for measuring similarity. Hafemman et al. in a series of publications, proposed methods for learning features from images. Specifically, the authors in [38] introduced a formulation for learning features from genuine signatures by a development dataset, and used them in order to train writer dependent classifiers to another set of users. In [64] the authors obtained state-of-the-art results on several GPDS datasets using CNN architecture and in [65] demonstrated a novel formulation that leverages knowledge of skilled forgeries for feature learning. Although SR methods have not been exploited for feature extraction in offline SV systems prior to [16] and [17], in [66] a method for writer identification based on sparse representation of handwritten structural primitives, called graphemes or fraglets was presented while in [67] an online signature verification technique based on discrete cosine transform (DCT) and sparse representation also appears. In addition, some sort of codebook formation have been also proposed in [68] by means of forming codebooks using signature samples of an independent database with the k-means algorithm and in [23] by creating a codebook of first order HOGs and then coding each feature to the nearest word in the codebook. Finally, as it said "whenever using k-means to get a dictionary, if you replace it with sparse coding it'll often work better" [69], and therefore our intuition to use SR is got stronger.

B. Overview of the proposed method

The proposed handwritten signature verification system is utilizing a sparse representation framework in order to learn local features and construct a global signature descriptor. The two main approximations of sparse coding (greedy and convex relaxation) and their efficiency are thoroughly investigated; along with multiple pooling strategies, Including a novel pooling function based on second order statistics. In addition, a widespread key-point selection algorithm is also employed in order to further emphasize salient locations across the signature.

The preprocessing stage of grayscale signature images consists of thresholding using Otsu's method [70], followed by the morphological process of thinning. In order to define the Optimal Thinning Level (OTL) at each signature, the patches from the binary/thinned images are considered. Patches are extracted from every pixel of the thinned signature's trace while the percentage of the signature pixels that inhabit each patch is also counted. This information helps to define the notion of patch density (PD) of a signature and plot it as a function of the number of successive thinning operations applied. In this way, an individual optimal thinning level (OTL) can be defined for each signature by utilizing the minimum value of its corresponding PD slope. Following the completion of this procedure for all reference samples, their

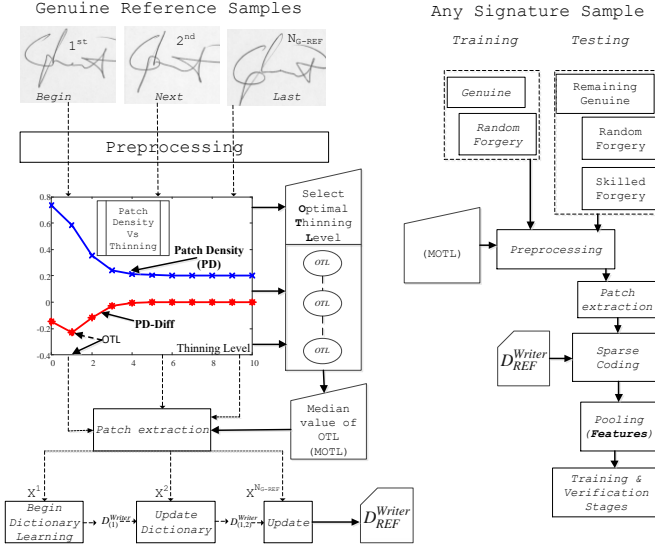


Fig. 1. A diagram of the very heart of the proposed pipeline. The sketch is emphasized on the preprocessing and dictionary learning stages. The Optimal Thinning Level (OTL) at the preprocessing stage is selected from the extreme point of the patch density slope (located at the upper center of the figure).

median value defines the writer optimal thinning level (MOTL) which will be used for the preprocessing of all the signature images corresponding to the writer under consideration.

For SR the patches are extracted from the grayscale signature image, at every position indicated by the skeleton of the signature, obtained via the thinning process. Subsequently, the gray values of the patches associated with the genuine reference samples are transformed into column vectors and used as input to a dictionary learning algorithm and then, for every signature, the patches are encoded in order to provide the sparse coefficients. The final feature of each signature image is formed by applying a pooling function on the sparse vectors, using a specially designed spatial pyramid, which segments the signature skeleton in equimass parts (i.e. with the same number of pixels).

Additionally, the key-points derived from the BRISK [71] algorithm pinpoint image regions of interest, whereas the sparse codes of the corresponding nearby patches are pooled together. The obtained pooled vector is concatenated with the spatial pyramid vector in order to form the final signature descriptor. Finally, the signature verification system is formed by a binary radial basis SVM classifier, which takes the above features as inputs and tries to discriminate the genuine signatures from forgeries. In the training of the classifier, the positive class is composed from the reference genuine signatures of the writer and the negative class from random forgery signatures, randomly sampled from a few of the remaining writers. Figure 1 presents a motif of the proposed system with emphasis on the preprocessing and the dictionary learning stage.

A. Sparse Coding

Informally, the objective of Sparse Representation (SR) is to encode a set of signals as a linear combination of a few elements of a predefined set (dictionary) whose elements are defined as basis vectors or atoms. The sparse dictionary is usually overcomplete i.e. the number of dictionary elements is higher than the input signal's dimensions. Several techniques for SR have been successfully applied in the fields of computer vision, pattern recognition and machine learning. The key idea is to represent an observed phenomenon through the activation of only as few components as possible. It has been shown that the V1 part of the brain which receives visual stimuli, is alleged to perform a similar process with sparsity objectives [25]. For an overcomplete dictionary $\mathbf{D} = [\mathbf{d}^1, \mathbf{d}^2, \dots, \mathbf{d}^K] \in \mathbb{R}^{n \times K}$ with $K > n$ and for M input signals $\mathbf{X} = [\mathbf{x}^1, \mathbf{x}^2, \dots, \mathbf{x}^M] \in \mathbb{R}^{n \times M}$, the formulation of SR is usually expressed with the following equivalent forms of regularized or constraint optimization problem expressed by (1) and (2) respectively:

$$\frac{1}{M} \sum_{i=1}^M \min_{\mathbf{a}^i} \left(\frac{1}{2} \|\mathbf{x}^i - \mathbf{D}\mathbf{a}^i\|_2^2 + \lambda \psi(\mathbf{a}^i) \right) \quad (1)$$

$$\frac{1}{M} \sum_{i=1}^M \min_{\mathbf{a}^i} \left(\frac{1}{2} \|\mathbf{x}^i - \mathbf{D}\mathbf{a}^i\|_2^2 \right), \text{ s.t.: } \psi(\mathbf{a}^i) \leq \rho, \forall_{i=1:M} \quad (2)$$

In the above expressions (1), (2), the matrix $\mathbf{A} = [\mathbf{a}^1, \mathbf{a}^2, \dots, \mathbf{a}^M] \in \mathbb{R}^{K \times M}$ represents the sparse coefficients for the M input signals, $\|\mathbf{x}^i - \mathbf{D}\mathbf{a}^i\|_2^2$ is the reconstruction error, λ is the regularizer parameter or Lagrange multiplier and $\psi(\bullet)$ is the sparsity-inducing term [72]. The embedded term $\psi(\bullet)$ is defined to be the l_p -norm (defined for $1 \leq p \leq \infty$) of the coefficients \mathbf{a}^i , i.e. $\psi(\mathbf{a}^i) = l_p(\mathbf{a}^i) = \|\mathbf{a}^i\|_p = \left(\sum_{j=1}^K (\mathbf{a}^i[j])^p \right)^{1/p}$ for a specific value of p . The most popular forms are the ones that rely on the l_0 -norm and l_1 -norm, i.e. for $p=0$ or $p=1$. Specifically, the l_0 -norm or pseudo-norm is equal to the count of non-zero elements ρ (sparsity level) of the representation vector \mathbf{a}^i , and so it is the most direct sparsity measure. However, this selection leads to a combinatorial NP-hard optimization problem, whose solution can only be approximated [26]. On the contrary, the l_1 -norm leads into a convex relaxation of the coding problem and has been proved that encourages sparse solutions [26]. Thus, the sparsity inducing term is usually utilized by the l_0 -norm which is a greedy non-convex approximation and the l_1 -norm which is a convex relaxation named Lasso [73].

To obtain a satisfactory solution of Sparse Coding with the use of the l_0 -norm regularization term, greedy algorithms can be utilized in order to seek and provide an approximate

optimized solution. The idea behind the greedy strategy is to always seek for the atom with the strongest relation to the sample under examination, in an effort to aggressively reduce the reconstruction error in the least-squares sense. The orthogonal matching pursuit (OMP) [74] along with a number of variations like regularized OMP, stage wise OMP, sparsity adaptive matching pursuit, are typical representatives of greedy algorithms. Given a dictionary \mathbf{D} and any sample \mathbf{x}^i , OMP sequentially selects the atoms with the highest correlation to the respective sample's residual. At a step $s: 0 < s \leq \rho$ the selected atom is given by: $k_s = \arg \max_j |(\mathbf{d}^j)^T \mathbf{r}_{s-1}|$, where \mathbf{r}_{s-1} is the current residual.

Once an atom is selected, the \mathbf{x}^i signal is projected onto the span of currently selected atoms as: $\hat{\mathbf{a}}_s = (\mathbf{D}_{V_s})^+ \mathbf{x}^i$, where $V_s = V_{s-1} \cup k_s$ is the set of indices pointing at the currently selected dictionary atoms, and \mathbf{D}_{V_s} is the subset of dictionary indexed by V_s . The new residual is now given by $\mathbf{r}_s = \mathbf{x} - \mathbf{D}_{V_s} \hat{\mathbf{a}}_s$ while the process now repeats until either ρ atoms are selected or the residual magnitude minimizes. In this work we utilized the batch-OMP implementation [75], which makes use of Cholesky decomposition in order to reduce the computational cost of repeated re-projections, as a means to assess the efficiency of greedy SR methods in signature verification.

The use of the l_1 -norm, has been also broadly proposed for sparse solutions since it provides an analytical solution and can be solved in polynomial time. Solvers for handling the l_1 -norm oriented SR problems, include the well-known basis pursuit [76] and the Lasso [73] among others. A number of methods for solving the l_1 -norm problems rely on coordinate descent methods, which have been found to be efficient enough in cases where dictionary atoms exhibit low correlation. Unlike, when the atoms of the dictionary are highly correlated, homotopy-based methods can be applied. The homotopy methods solve the regularized sparse coding optimization problem, as expressed by (1), and track the entire regularization path (i.e. the solutions for all possible values of λ), like the least angle regression (LARS-Lasso) algorithm [77]. The LARS-Lasso algorithm calculates the solution path by repeatedly decreasing the value of λ and using as a warm-start of the previously calculated solution. The uniqueness of the solution for a specific value of the parameter λ , i.e. the existence of a single normalized path solution, is ensured and it can be proved that the solution path is piecewise linear [78]. This property is very important since the algorithm follows the direction of each segment until it reaches a critical point, i.e. where either a non-zero element becomes zero (so it is removed from the active set of coefficients) or a new non-zero element is added to the active set of coefficients. Therefore, the homotopy method initializes with an empty set of coefficients, and iteratively updates it by one variable at a time. The complexity of the method relies in reversing the

covariance matrix of the selected atoms at each critical point in order to update the active set of coefficients, which is performed by the Cholesky decomposition or the Woodbury formula. In this work the LARS-Lasso algorithm, which is a part of the SPAMS toolbox [78], has been utilized to investigate the efficiency of sparse coding with convex relaxation.

B. Dictionary Learning

The most efficient way for dictionary construction is through a learning process that enables the dictionary (i.e. atoms) to be fitted to the input-training data. The most common dictionary learning methods are unsupervised and have been mainly utilized for image processing problems, such as image compression and super resolution. Although these methods are not explicitly enforcing discriminative behavior to the sparse coefficients since the cost function relies only on reconstruction error, they have been used for classification tasks with remarkable results [79]. The sparse representation problem (i.e. dictionary learning and sparse coding) is a joint optimization problem with respect to dictionary \mathbf{D} as well as the coefficients $\mathbf{A} = \{\mathbf{a}^i\}$ and it is expressed as follows:

$$\min_{\mathbf{D} \in C, \mathbf{A} \in \mathbb{R}^{K \times M}} \left(\frac{1}{2} \|\mathbf{X} - \mathbf{D}\mathbf{A}\|_F^2 + \lambda \|\mathbf{A}\|_p \right) \quad (3)$$

$$\min_{\mathbf{D} \in C, \mathbf{A} \in \mathbb{R}^{K \times M}} \left(\frac{1}{2} \|\mathbf{X} - \mathbf{D}\mathbf{A}\|_F^2 \right) \text{ s.t.: } \|\mathbf{A}\|_p \leq \rho \quad (4)$$

where the set C of the dictionary atoms is usually defined to be the convex set of matrices that satisfy the following constraint: $C \triangleq \{\mathbf{D} \in \mathbb{R}^{n \times K} \text{ s.t.: } \forall_{j=1:M}, (\mathbf{d}^j)^T \mathbf{d}^j \leq 1\}$ in order to avoid large values, which consequently might lead to arbitrarily small values for the coefficients.

The greedy approximation of l_0 -norm regularized SR is addressed in this work by means of the KSVD [80, 81] and the associated OMP algorithm for dictionary learning and sparse coding respectively. For the convex relaxation approach, the online learning method [78] along with the LARS-Lasso algorithm have been employed for the corresponding tasks. In the case of the KSVD/OMP algorithm pair, the notation of eq. (4) has been selected due to the fact that the use of the ℓ_0 sparsity constraint $\|\mathbf{A}\|_0 \leq \rho$ with $\rho \in \mathbb{N}^+$, intuitively assigns as a design parameter the integer number of the non-zero elements ρ . On the other hand, for the case of online/LARS-Lasso algorithm pair the notation of eq. (3) has been followed due to the fact that the interpretation of the parameter $\rho_1 \in \mathbb{R}$ in the ℓ_1 constraint $\|\mathbf{A}\|_1 \leq \rho_1$ does not provide any thoughtful intuition regarding the sparsity of the atoms as a design parameter. Instead, the parameter λ of eq. (3) shall be used as the design parameter of the method which now controls the sparsity. From a theoretical point of view, for an appropriate dictionary, the solution obtained with the use of the l_1 -norm is

equivalent to the one provided by another l_0 -norm based solution with full probability [82, 83], [26]. However, this l_1 / l_0 equivalence phenomenon, does not hold in the case of the joint regularized and constrained dictionary learning problem since it has been reported that different formulations of the dictionary learning problem do not admit the same solutions even for the case of using the same l_1 -norm [78]. That is the reason behind our decision to evaluate the performance of both l_0 and l_1 -norm approaches.

IV. FEATURE EXTRACTION

A. Preprocessing

Preprocessing consists of three steps: binarization followed by thinning, and finally patches extraction. During thinning, successive morphological operations are applied on the original binary image in order to provide a gradual skeletonization of the signature. Intuitively, the outcome of the thinning operation affects the verification performance since it modifies the shape of the signature image. It has been experimentally observed that the thinning level is critical for a Signature Verification (SV) system's performance and its optimal value is not the same for all databases [18]. This work proposes a novel method for selecting the optimal thinning level (OTL) for each signature and consequently for each writer. The OTL is defined to be the number of thinning operations that results to the steepest descend of the density function, as mentioned in section 2.2. Following the enrollment of a set of genuine reference signatures for a person, its median value of the associated OTL values (MOTL) accompanies the design of the model for each writer, i.e. $MOTL(N_{G-REF}) = median(OTL(i)), i \in [1, \dots, N_{G-REF}]$. Hence, for any input signature which claims an identity, the number of thinning operations will be determined by the MOTL value of the signing person. Algorithm 1 outlines the calculation of OTL and MOTL for a set of reference images of one writer.

Figure 3 presents the corresponding plots of the a) patch density, b) patch density derivative, expressed by its associated patch density difference and c) OTL-MOTL values for one writer and an indicative number of his/hers genuine samples derived for all the signature datasets namely CEDAR, MCYT-75, GPDS300 and UTSIG. A comment on the extracted results reveals that the genuine signatures that are part of the CEDAR dataset have the majority (~95%) of their OTL values to be equal to one with few (~5%) signature samples having their OTL values to two. For the MCYT-75 dataset the majority of their OTL values are equal to two with very few samples having their OTL values to three and four. For the GPDS300 dataset, the OTL values appear to distribute between 2-5, with an observed mode of 4, while for the UTSIG dataset the OTL values have been found to distribute equally to the values 2 and 3. Especially for the CEDAR and MCYT-75 datasets, figure 3 indicates that they are more stable in terms of acquisition conditions comparing to the GPDS300

Algorithm 1: Define optimal thinning level for a reference set of genuine signatures.

Require: $B_p, i=1:N_{G-REF}$ -Reference binary set of images, the output of the binarization step, N_p -patch size.

```

1: for  $i=1:N_{G-REF}$ 
2:   set  $th\_lev = 0$  (thinning level)
3:   Repeat
4:      $TH_{th\_lev}^i = THIN\_OPERATION(B_i, th\_lev)$ 
5:     Create map with locations of  $TH_{th\_lev}^i$  signature pixels.
6:     for  $j =$  each signature pixel of the map
7:       Impose a  $N_p \times N_p$  patch, centered at the coordinates of the  $j$ -pixel.
8:       Measure the number of signature pixels that reside in the patch. ( $local\_patch\_density$ )
9:       Normalize by  $N_p \times N_p$  and ASSIGN value to LD( $j$ ).
10:    end for
11:    Evaluate mean value of LD and ASSIGN value to PD( $th\_lev$ ).
12:     $th\_lev \leftarrow th\_lev + 1$  (increase thinning level)
13:  Until  $TH_{th\_lev}^i = TH_{th\_lev+1}^i$  (has idempotent stage reached?)
14: Find minimum of the difference of the PD function, RETURN minimum index to OTL( $i$ ).
15: end for
Return: MOTL: The median value of OTL; characterization of the reference samples.

```

Fig. 2. Algorithm for the calculation of the Optimal Thinning Level (OTL). The MOTL is the median value of OTL.

and UTSIG dataset. Thus one could consider the SV problem addressed by CEDAR and MCYT-75 dataset to resemble a case study in which the aspect ratio and acquisition conditions do not vary significantly, similar to situations encountered in mobile banking applications.

B. Patch Extraction

The signature patches are extracted from the original grayscale signature image and are designated by the signature's skeleton after the thinning operation. Specifically, the patches' centers are located at every pixel of the signature skeleton, thus the number of image patches equals the number of pixels in the signature's skeleton. Moreover, the patches are centered, i.e. have their average intensity been subtracted in order to have a zero mean value. The centering of each patch produces data invariant to the mean intensity and the learned structures, like edges, are anticipated to have zero mean as well. In all the conducted experiments the patch size has been set to five i.e. $n=25$. Our main rationale behind this selection is to keep the complexity of the local manifold of patches reasonably low. The reason is that sparse codes of data lying on smoother and more uniform manifolds tend to create more evenly distributed coefficients along the codebook's elements. Such cases are less prone to the phenomenon where very few dictionary elements are over-represented in the resulting sparse codes and are responsible for a significant amount of the total energy, thus predominantly shaping the distance between global image descriptors formed by these codes and requiring special pooling strategies [84] to restore the discriminative power.

With this aim, it is valuable to consider the parameters which affect the dimensionality and shape of the underlying local manifolds. In [85] Peyré shows that the local manifold of patches from cartoon images (images that contain sharp variations along regular curves) can be parameterized by two variables, leading to a manifold topologically equivalent to the surface of a cylinder in 3D space. This parameterization holds as long as the signal within each patch can be approximated by

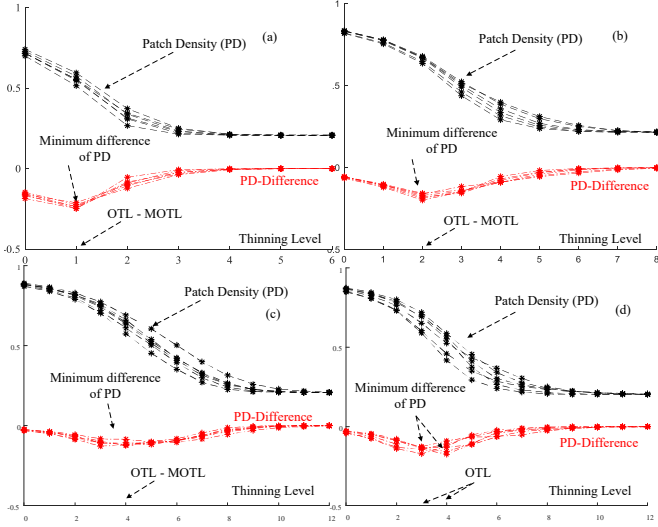


Fig. 3. Plots of the Patch Density (PD) and of the associated differences (differences of PDs) as a function of the thinning level. The above plots are demonstrated for one writer and an indicative set of six genuine samples derived from the (a) CEDAR, (b) MCYT-75, (c) GPDS300 and (d) UTSIG signature datasets. The patch size has been set to 5.

two regions (black and white) separated by a linear segment. If the patch size become larger and the edges within the patches appear curved, extra degrees of freedom have to be included to the signal's model thus leading to a more complex manifold. Similarly to cartoon images, the nature of the signal within signature patches is such that can be modeled by a handful of parameters if the patch size is small-enough, indicating a low-dimensional underlying manifold structure, but the complexity can be dramatically increased if the patch becomes big enough to contain curves and parts from neighboring line segments. We set patch size equal to 5, since it is a good tradeoff to the underlying signal's complexity-since for smaller patches the local manifold obviously becomes degenerate- and also to the overall computational complexity, which is dictated by the dictionary size whose over-completeness requirement points back to the patch dimensionality as the most significant parameter. It is worth noting that this scale of patches has also proven to be efficient in previous research efforts [18] on the particular problem, delivering state-of-the-art results and strengthening our decision on this selection.

C. SR-driven local feature extraction

As already mentioned, the dictionary $\mathbf{D}_{NG-REF}^{writer}$ (or \mathbf{D} for simplicity) is considered to represent the characteristic properties of the signatory. The patches extracted from one signature are represented as columns of the matrix $\mathbf{X} \in \mathbb{R}^{n \times M}$ and the dictionary for sparse representation is updated via an inventive process, in which the patches of one reference signature are used in each update and ultimately, all the reference signatures are utilized in a cascade fashion. Hence, dictionary is updated consecutively using each one of the writer's genuine reference signatures. Thus, the system can integrate easily a new reference genuine signature of the writer

and thus, it is practical for application in everyday scenarios. Figure 4, presents four different reference dictionary examples from the four datasets we use. Following the construction of the dictionary, for every inserted signature image its patches are extracted and encoded using the dictionary and SR coding in order to obtain the sparse representation matrix \mathbf{A} . Depending on the case, the dictionary learning and the sparse coding are implemented with either the K-SVD/OMP or SPAMS/LARS-Lasso algorithm pairs. In addition, the impact on the system performance of some other popular optimization constraints has been also explored with priors such as the positivity constraint of the coefficients, the non-negativity constraint for the dictionary atoms and the non-negative matrix factorization (NMF) method in which the matrix \mathbf{D} and the vectors \mathbf{A} are required to be positive. For the cases in which \mathbf{D} is positive, the SPAMS/LARS-Lasso algorithm has been invoked but without the centering procedure of patches.

The operating parameters of the KSVD/OMP algorithms were set as follows: number of maximum iterations $t_{max} = 50$, number of atoms was set to $K = 60$ in order to ensure the over-completeness (as a rule of thumb we use a number of atoms greater than twice the patch size dimension) and $\rho = 3$ for the sparsity level in order to provide a total 5% sparsity on the coefficients. For the case of the online/LARS-Lasso case, the operating parameters were also set as follows: number of atoms $K = 60$ (same as the KSVD/OMP), number of signals drawn at each iteration or mini-batch size $\eta = 512$, while the dictionary learning algorithm was allowed to run for a typical execution time of one minute, a time which is considered adequate for the size of the signature patches. In addition, the regularization parameter λ was set to 0.15, a value which is in proximity to the classical $1/\sqrt{n}$ normalization factor proposed by Bickel et al. [86]. Figure 5 illustrates the SR concept as it is applied in the proposed method for signature modeling.

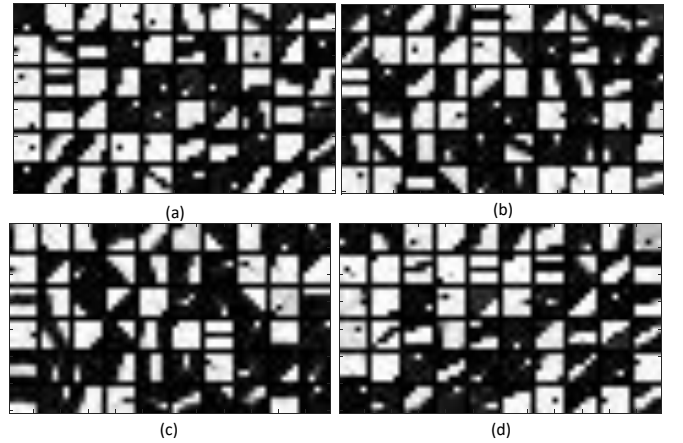


Fig. 4. Examples of sparse representation Dictionaries for one writer of (a) CEDAR, (b) MCYT-75, (c) GPDS300 and (d) UTSIG signature datasets. Each dictionary is composed of sixty atoms, that are represented as image patches of 5 x 5 pixels, on a 6 x 10 image grid.

D. Pooling Strategies

It is common for contemporary computer vision algorithms to incorporate a pooling stage, which aggregates local features over a region of interest [87], [21] [88]. In this work, the simplest variant of the final signature descriptor which is evaluated stems from the global aggregation of the local patch sparse coding coefficients into a final vector, through an appropriate pooling function. Depending on the pooling function, the corresponding signature descriptor is denoted hereafter as $f_I^{F1} - f_I^{F5}$ and defined as follows:

- F1: Average

$$f_I^{F1} = \{f_I^{F1}[j]\} = \left\{ \frac{1}{M} \sum_{i=1}^M \alpha^i[j] \right\}, j = 1:K \quad (12)$$

- F2: Max

$$f_I^{F2} = \{f_I^{F2}[j]\} = \max(\alpha^i[j]), i = 1:M, j = 1:K \quad (13)$$

- F3: Standard deviation

$$f_I^{F3} = \{f_I^{F3}[j]\} = \left\{ \sqrt{\frac{\sum_{i=1}^M (\alpha^i[j] - f_I^{F1}[j])^2}{M-1}} \right\}, j = 1:K \quad (14)$$

- F4: Sum normalization

$$f_I^{F4} = \{f_I^{F4}[j]\} = \frac{\sum_{i=1}^M \alpha^i[j]}{\sum_{j=1}^K \sum_{i=1}^M \alpha^i[j]}, j = 1:K \quad (15)$$

- F5: l^2 - normalization:

$$f_I^{F5} = \{f_I^{F5}[j]\} = \frac{\sum_{i=1}^M \alpha^i[j]}{\sqrt{\sum_{j=1}^K \left(\sum_{i=1}^M \alpha^i[j] \right)^2}}, j = 1:K \quad (16)$$

Average pooling is the simplest pooling function that estimates the average SR coefficients from the whole region of interest. The max pooling operation only captures the most salient representation value from the entire region of interest. Standard deviation is proposed here as an alternative pooling function that captures 2nd order statistics of the coefficients' distribution, in an aim to investigate if this type of information can deliver better discrimination capabilities to the resulting descriptor. Normalized Sum pooling function produces vectors with intensity invariance qualities, and finally the l^2 normalized function produces vectors projected onto the unitary ball, which can be important for linear classification kernels [87].

Given the fact that the number of dictionary atoms is K , it follows easily that the final feature vector's dimensionality provided by the preceding pooling operations also equals to K . In order to encapsulate local signature information to the final feature vector, a specially designed Spatial Pyramid is employed for segmenting the signature images into a grid of

$(\beta \times \beta)$ sub-regions. For each $I_\beta(t)$, $t = 1:\beta^2$ segment of this pyramid, its selected $\mathbf{x}_{I_\beta^2(t)}$ patches are enabled for indexing the local $\alpha_{I_\beta^2(t)}$ representation coefficients, which in their turn are subjected to the same pooling operations $F(\mathbf{A}_{I_\beta^2(t)})$ that were used for the computation of the $f_I^{F1} - f_I^{F5}$ global versions. As an aftermath, the dimensionality of the expanded feature $f^{Fg} = \{f_I^{Fg}, f_{I_\beta^2}^{Fg}\}$, $g = 1:5$, now equals to $(\beta^2 + 1) \times K$. In this work the value for the β parameter has been set to two and three, i.e. (2×2) and (3×3) equimass sub-regions for the spatial pyramid.

E. Emphasizing into informative local keypoints

A human expert, who wishes to analyze a signature image in order to verify if it is genuine or forgery, focuses at certain points of the signature. In an effort to discover these signature's points of interest we utilize the saliency-modeling mechanism implemented by the Binary Robust Invariant Scalable Keypoints (BRISK) [71]. BRISK have the advantage of dramatically lowering computational complexity and thus are suited for low power devices, such as practical portable SV systems. BRISK computation relies on an easily configurable circular sampling pattern from which it computes brightness comparisons to form a binary 512 bit descriptor string and estimates keypoint scale in continuous scale-space. In this work only the detected keypoint locations and not the keypoint descriptors (BRISK) are utilized. Hence, keypoints indicate the patches, and thereafter the corresponding Sparse Codes will be pooled together in order to obtain an additional feature vector. This vector is concatenated with the spatial pyramid vector and in this way, the final feature dimensionality is $(\beta^2 + 2) \times K$. Figure 6, depicts a zoomed area of an example signature image where the BRISK keypoints and their nearest signature pixels are denoted as crosses and points, respectively. The final feature vector can be expressed as: $f^{Fg} = \{f_I^{Fg}, f_{I_\beta^2}^{Fg}, f_{I_{BR}}^{Fg}\}$.

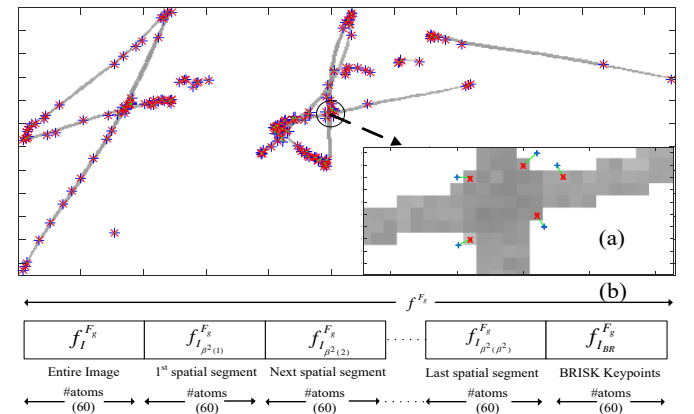


Fig. 6. a) The BRISK keypoints are located on the trace of one signature. In the detail image, the (+) depicts the BRISK actual coordinates while the (x) mark the assigned nearest signature pixel neighbors. b) Structural configuration for the f^{Fg} feature vector. In this example, the number of atoms has been set to 60.

V. EVALUATION

A. Datasets and Experimental Protocols

Four signature datasets were used in order to test the proposed system architecture. A short description is provided here. The first one is the popular CEDAR dataset [89]. For each one of the 55 enrolled writers, a total of 48 signature specimens (24 genuine and 24 simulated) confined in a 50 mm by 50 mm square box were provided and digitized at 300 dpi. The simulated signatures found in the CEDAR dataset are composed from a mixture of random, simple and skilled forgeries. The second signature dataset used was the off-line version of the popular MCYT signature database [36, 90]. A whole of 30 signature samples (15 genuine and 15 simulated) signature samples were recorded for each one of the 75 enrolled writers at a resolution of 600 dpi and for and the capture area is 127×97 mm. Both CEDAR and MCYT-75 datasets have their samples confined within one bounding box. The third signature dataset was the GPDS300 [36, 42] which contains 24 genuine signatures and 30 simulated forgeries of 300 individuals stored in an 8-bit, grey level format. A special feature of this dataset is that the acquisition of signature specimens was carried out with the aid of two different bounding boxes of size 5×1.8 cm and 4.5×2.5 cm respectively. As a result, the files of this dataset include images having two different aspect ratios; this phenomenon conveys a structural distortion highlighted during the feature extraction procedure. The fourth signature dataset is the Persian UTSIG, which was created by Soleimani et al. [91]. It contains specimens from 115 writers where each one has 27 genuine signatures, 3 opposite-hand signatures, and 42 skilled forgeries made by 6 forgers. As stated by the dataset creators, a property of the UTSIG dataset, compared with the other public and popular ones, is that UTSIG has more samples, more classes, and more forgers. An important characteristic of the UTSIG is that the acquisition of signature specimens was carried out with the aid of six different bounding box sizes simulating real world conditions and public services application forms.

Since this work addresses writer depended signature verification, for any signatory a specific model is created by randomly employing N_{G-REF} genuine reference signature samples. The number of N_{G-REF} has been primarily set to five (5) for addressing cases in which only a few samples are available. In order to provide comparable results with other state-of-the-art methods, we allowed the N_{G-REF} parameter to assume values from 5 and/or 12 according to the specific needs of each dataset. A number of methods exist in order to quantify the efficiency of the proposed system. The false acceptance rate FAR and its associate probability P_{FAR} depicts a system's measure of the resistance to input samples other than the genuine ones like random or skilled forgeries. On the other hand, the false rejection rate FRR and its accompanied probability rate P_{FRR} provides a system's measure of the

failure to genuine samples. These operating system parameters are computed as a function of a sliding threshold whose extremes are located between the minimum and maximum values of the cross-validation SVM output scores CVS^{\oplus} . A number of methods exist in the literature in order to quantify the efficiency of the proposed system. Some examples include independent experiments and corresponding solutions like: a) the P_{FAR}^S vs P_{FRR} , where the upper script S denotes skilled forgery, along with their average AVE^S or equal error rates: $EER^S : P_{FAR}^S = P_{FRR}$, and b) the P_{FAR}^R vs P_{FRR} , where the upper script R denotes random forgery, along with their corresponding average AVE^R or equal error rates $EER^R : P_{FAR}^R = P_{FRR}$. Other methods provide joint solutions [51], [16], [17], which initially evaluate the $TH^{\oplus EER^S}$ - threshold, defined as the value which designates the EER^S operating point and then, taking into account this value in order to assess the $P_{FAR}^{R \oplus EER^S}$ error rate.

At this point we feel the need to justify our choice of metrics. Researchers suggest handling SV as either a one class pattern recognition problem or a two class pattern recognition problem. The issue arises from the fact that the negative class of the test set has representatives from both skilled and random forgery samples. The key point is that the skilled forgery class is composed of few samples compared with the random class. So, if one tries to incorporate both forgery populations there is always the danger of reporting biased results. For example, reporting an EER point of $EER^{R \& S} : \{P_{FAR}^{R \& S}\} = P_{FRR}$ where all types of forgery samples are employed; this is clearly biased since the forgery class has samples with two different populations of forgery. In this paper, as in [16], [17], the $EER_{user-threshold}^S$ was used by employing user-specific decision thresholds in order to evaluate the verification performance of the proposed system. Also the calculation of the P_{FAR}^S, P_{FRR} rates with the utilization of a predetermined threshold (i.e. hard decisions) is provided with a-priori knowledge of the cross validation procedure scores CVS^{\oplus} . Specifically, this hard threshold value corresponds to the 50% of the average of the genuine CVS^{\oplus} scores for each writer. For completeness, at this specific threshold point the P_{FAR}^R error rate is evaluated by employing the genuine samples of the remaining writers from the test set.

VI. EXPERIMENTAL RESULTS

For the sake of sanity and in order to avoid a deployed ocean of exhausting scenarios for all datasets, complete results are provided in Tables 1-6 which involve the popular CEDAR and MCYT-75 datasets. All the experimental protocols were repeated ten times and the results were averaged in order to provide meaningful comparisons.

TABLE 1
Verification Error Rates (%) for the CEDAR signature dataset with
 l_0 -norm (KSVD/OMP).

Pooling Function F(A)	SP : $\beta = 2$ (Dim=360)				SP : $\beta = 3$ (Dim=660)			
	P_{FAR}^S	P_{FRR}	EER^S	$P_{FAR}^{R \otimes EER^S}$	P_{FAR}^S	P_{FRR}	EER^S	$P_{FAR}^{R \otimes EER^S}$
F1	6.83	7.32	2.67	0.43	6.13	7.18	2.80	0.27
F2	9.45	9.83	4.17	2.93	8.83	8.65	3.21	0.76
F3	4.76	4.91	1.44	0.17	4.78	5.63	1.80	0.12
F4	8.12	9.94	7.51	1.95	12.7	20.2	13.4	4.82
F5	5.31	5.27	3.08	0.35	5.05	5.11	2.48	0.24

Number of reference training samples $N_{G-REF} = 5$. The EER^S rate corresponds to the user specific threshold case.

TABLE 2
Verification Error Rates (%) for the MCYT-75 signature dataset with
 l_0 -norm (KSVD/OMP).

Pooling Function F(A)	SP : $\beta = 2$ (Dim=360)				SP : $\beta = 3$ (Dim=660)			
	P_{FAR}^S	P_{FRR}	EER^S	$P_{FAR}^{R \otimes EER^S}$	P_{FAR}^S	P_{FRR}	EER^S	$P_{FAR}^{R \otimes EER^S}$
F1	10.4	7.32	3.80	0.22	9.18	7.12	3.19	0.14
F2	14.7	14.6	10.9	3.16	15.6	11.5	8.65	1.12
F3	8.09	6.75	3.18	0.16	8.07	6.21	2.82	0.07
F4	12.99	16.17	10.8	3.08	11.0	23.7	16.7	6.17
F5	7.64	7.76	3.23	0.14	7.77	7.92	3.46	0.13

Number of reference training samples $N_{G-REF} = 5$. The EER^S rate corresponds to the user specific threshold case.

TABLE 3
Verification Error Rates (%) for the CEDAR signature dataset with
 l_1 -norm (ONLINE/LARS-LASSO).

Pooling Function F(A)	SP : $\beta = 2$ (Dim=360)				SP : $\beta = 3$ (Dim=660)			
	P_{FAR}^S	P_{FRR}	EER^S	$P_{FAR}^{R \otimes EER^S}$	P_{FAR}^S	P_{FRR}	EER^S	$P_{FAR}^{R \otimes EER^S}$
F1	6.99	7.60	2.65	0.37	6.59	6.61	3.08	0.23
F2	9.42	9.71	3.45	1.55	8.52	8.01	2.80	0.48
F3	4.61	4.64	1.62	0.12	4.88	5.81	2.01	0.08
F4	8.19	8.73	3.52	0.56	9.17	8.71	3.97	0.41
F5	7.05	7.81	3.38	0.41	5.49	6.48	3.07	0.22

Number of reference training samples $N_{G-REF} = 5$. The EER^S rate corresponds to the user specific threshold case.

TABLE 4
Verification Error Rates (%) for the CEDAR signature dataset with
 l_1 -norm (ONLINE/LARS-LASSO).

Pooling Function F(A)	SP : $\beta = 2$ (Dim=360)				SP : $\beta = 3$ (Dim=660)			
	P_{FAR}^S	P_{FRR}	EER^S	$P_{FAR}^{R \otimes EER^S}$	P_{FAR}^S	P_{FRR}	EER^S	$P_{FAR}^{R \otimes EER^S}$
F1	10.46	8.57	3.91	0.24	7.82	7.68	3.58	0.14
F2	15.8	14.3	11.20	3.09	13.9	12.3	8.60	1.08
F3	8.35	7.58	3.71	0.22	7.59	7.29	3.40	0.10
F4	12.2	13.43	3.93	0.30	9.82	9.68	3.53	0.15
F5	7.87	7.59	3.66	0.20	7.07	7.69	3.05	0.12

Number of reference training samples $N_{G-REF} = 5$. The EER^S rate corresponds to the user specific threshold case.

It can be noticed that the verification error rates for the CEDAR and MCYT datasets do not vary substantially when both l_0 and l_1 -norms dictionary learning and SR are used. This is in accordance to the material exposed to section 3.2 which states that for a given dictionary \mathbf{D} both l_0 and l_1 oriented SR solutions are equivalent, for some specific values of the design parameters ρ and λ . Of course, the problem of locating the appropriate value for these design parameters is not a trivial one since it depends on the individual signature characteristics. An additional issue that arises is that tuning the

system to a specific value either for ρ or λ depends mainly upon the different training modes. For example, suppose that one trains the proposed system with genuine as well as random forgeries with several values of the sparsity level ρ . It has been also observed during the conducted experiments that the cross validation procedure, which is used for the selection of the optimal classifier parameters, is almost ineffective against skilled forgeries. A potential solution could emerge by employing WI systems with skilled forgeries which are not assigned to any specific person during the training [65]. However, this approach is out of the scope of the present work.

The experimental outcomes have also shown that the best results for the CEDAR dataset are obtained with the use of a spatial pyramid with $\beta = 2$ while for the MCYT-75 the optimal results are obtained with the use of a spatial pyramid with $\beta = 3$. This is probably due to the fact that CEDAR signature specimens have been scanned with a resolution of 300dpi, while the MCYT-75 ones with a resolution of 600dpi, thus it is natural to expect that more pixels exist in the MCYT-75 segments. It should be noticed that, for the CEDAR dataset even when the spatial pyramid with $\beta = 2$ is used, there were a few patches in some segments, which profoundly did not provide any sort of discriminatory information, something that has not been encountered in the case of the MCYT-75.

An important result that arises from our experimental results is that the accuracy for the F3 pooling function (i.e. standard deviation) seems to outperform all other pooling functions in almost all cases. It is also interesting that although the use of F2 feature has been reported to perform quite well in all other computer vision applications, this is not the case for signatures images. A possible explanation relies on the very nature of the signature images which are a particular class of image signals that exhibit a degenerate structure. Since all signature images essentially share a limited set of structural elements, the resulting sparse coefficients of different signatures may not differ sufficiently in a 1st order statistic sense, as being the case in more complex image structures. Therefore, it is reasonable to deduce that higher-order statistics can deliver a better level of discrimination between the respective distributions of sparse coefficients, resulting into better verification performance. For further investigation we selected the spatial segmentation that corresponds to the best results, i.e. $\beta = 2$ for the CEDAR and $\beta = 3$ for the MCYT-75, and the l_1 -norm. Tables 5-6 provide comparisons with exactly the same reference and training samples for the following priors: a) the positivity constraint of the \mathbf{A} coefficients, b) the 'non-negative' \mathbf{C}' constraint for the dictionary atoms and c) the NMF method. The derived results indicate that none of these priors seems to provide any sort of significant improvement to the verification error.

Thus, for the GPDS300 signature dataset and given the l_1/l_0 equivalence, we will remain to the (l_0) norm KSVD/OMP dictionary learning and SR. Table 7, provides the corresponding results.

TABLE 5
Verification Error Rates (%) for the CEDAR signature dataset with l_1 -norm (ONLINE/LARS-LASSO) for the following priors:

- I. Positivity constraint of the A Coefficients,
- II. 'Non-Negative' C' constraint for the Dictionary Atoms and
- III. NMF method.

Pooling Function F(A)	A positive				C' dictionary constrains				NMF			
	P_{FAR}^S	P_{FRR}	EER^S	$P_{FAR}^{R \otimes EER^S}$	P_{FAR}^S	P_{FRR}	EER^S	$P_{FAR}^{R \otimes EER^S}$	P_{FAR}^S	P_{FRR}	EER^S	$P_{FAR}^{R \otimes EER^S}$
F1	7.26	7.99	2.38	0.29	7.29	7.72	2.43	0.34	9.13	8.41	2.22	0.39
F2	9.56	9.07	3.19	1.52	9.32	9.84	3.63	1.72	22.5	24.2	16.3	13.3
F3	4.74	4.92	1.77	0.15	4.97	4.96	1.71	0.26	6.48	9.41	1.52	1.09
F4	10.3	9.69	3.91	0.45	10.3	9.94	3.00	0.45	12.7	10.3	3.05	1.04
F5	9.98	7.69	3.17	0.35	9.83	9.99	2.78	0.32	9.78	9.36	2.64	0.54

Number of reference training samples $N_{G-REF} = 5$. Parameter of SP $\beta=2$.

The EER^S rate corresponds to the user specific threshold case.

TABLE 6
Verification Error Rates (%) for the CEDAR signature dataset with l_1 -norm (ONLINE/LARS-LASSO) for the following priors:

- I. Positivity constraint of the A Coefficients,
- II. 'Non-Negative' C' constraint for the Dictionary Atoms and
- III. NMF method.

Pooling Function F(A)	A positive				C' dictionary constrains				NMF			
	P_{FAR}^S	P_{FRR}	EER^S	$P_{FAR}^{R \otimes EER^S}$	P_{FAR}^S	P_{FRR}	EER^S	$P_{FAR}^{R \otimes EER^S}$	P_{FAR}^S	P_{FRR}	EER^S	$P_{FAR}^{R \otimes EER^S}$
F1	12.6	8.96	4.71	0.31	11.1	10.6	5.53	0.44	10.2	10.9	4.34	0.45
F2	19.4	18.3	12.4	3.43	18.8	19.4	11.9	2.50	30.8	30.4	24.3	20.3
F3	12.2	8.44	4.97	0.22	10.9	9.67	4.86	0.33	13.4	12.9	7.99	1.78
F4	14.4	11.3	5.38	0.59	13.6	14.1	5.34	0.45	17.2	18.1	6.69	1.98
F5	11.3	10.2	4.69	0.35	11.4	10.2	4.97	0.27	11.8	1.6	4.48	0.37

Number of reference training samples $N_{G-REF} = 5$. Parameter of SP $\beta=3$.

The EER^S rate corresponds to the user specific threshold case.

TABLE 7
Verification Error Rates (%) for the CEDAR signature dataset with l_0 -norm (KSVD/OMP).

Pooling Function F(A)	SP : $\beta = 2$ (Dim=360)				SP : $\beta = 3$ (Dim=660)			
	P_{FAR}^S	P_{FRR}	EER^S	$P_{FAR}^{R \otimes EER^S}$	P_{FAR}^S	P_{FRR}	EER^S	$P_{FAR}^{R \otimes EER^S}$
F1	6.91	6.22	2.47	0.59	6.46	6.47	3.14	0.44
F2	8.27	8.89	3.98	3.70	11.79	9.37	4.43	1.82
F3	6.73	6.13	1.50	0.33	5.01	5.92	1.97	0.19
F4	16.1	19.3	15.2	6.23	18.6	29.4	20.4	10.0
F5	7.79	7.96	3.30	0.55	7.58	6.83	3.53	0.30

Number of reference training samples $N_{G-REF} = 5$. The EER^S rate corresponds to the user specific threshold case.

As it is observed, the F3 feature (standard deviation) still outperforms all other types. The increase of the spatial pyramid size from two to three does not provide any considerable verification improvement, except for the random forgery error as it is expressed from the P_{FAR}^R rate. We believe that this effect can be explained due to the indiscriminately nature of the spatial pyramid equimass segmentation which does not take into account the two different aspect ratios of the bounding box. As mentioned earlier, the UTSIG dataset is, according to the author's opinion, a significant realization step towards the assessment of situations which resemble typical conditions and constraints that are broadly encountered in daily transactions. Table 8 presents the results.

As expected, the provided verification results are poor regarding to the rates of the previous datasets however a closer look to P_{FAR}^R indicates that most likely the $N_{G-REF} = 5$ is not adequate in this case due to the large number of bounding box

TABLE 8
Verification Error Rates (%) for the UTSIG signature dataset with l_0 -norm (KSVD/OMP).

Pooling Function F(A)	SP : $\beta = 2$ (Dim=360)				SP : $\beta = 3$ (Dim=660)			
	P_{FAR}^S	P_{FRR}	EER^S	$P_{FAR}^{R \otimes EER^S}$	P_{FAR}^S	P_{FRR}	EER^S	$P_{FAR}^{R \otimes EER^S}$
F1	18.3	16.9	11.7	1.91	16.9	12.4	9.82	1.94
F2	25.3	21.6	17.0	7.02	23.6	15.7	13.35	3.33
F3	16.1	13.4	9.94	1.27	15.8	12.5	8.56	1.25
F4	24.5	27.6	21.1	6.39	29.8	29.5	25.15	12.5
F5	20.7	24.6	12.2	1.48	17.3	15.2	10.48	0.92

Number of reference training samples $N_{G-REF} = 5$. The EER^S rate corresponds to the user specific threshold case.

TABLE 9
Verification Error Rates (%) for the UTSIG signature dataset with l_0 -norm (KSVD/OMP).

Pooling Function F(A)	SP : $\beta = 2$ (Dim=360)				SP : $\beta = 3$ (Dim=660)			
	P_{FAR}^S	P_{FRR}	EER^S	$P_{FAR}^{R \otimes EER^S}$	P_{FAR}^S	P_{FRR}	EER^S	$P_{FAR}^{R \otimes EER^S}$
F1	13.6	13.5	8.13	0.53	12.1	9.37	7.33	0.25
F2	19.9	18.1	12.0	3.66	18.9	12.3	11.4	0.87
F3	13.2	11.5	7.36	0.33	9.77	8.17	6.22	0.12
F4	23.8	24.6	17.3	3.32	29.3	21.1	20.1	6.63
F5	13.9	12.7	8.51	0.39	10.1	9.55	7.44	0.21

Number of reference training samples $N_{G-REF} = 12$. The EER^S rate corresponds to the user specific threshold case.

sizes. Therefore, in accordance with the literature [91], [19] and for comparison purposes, we let the value of N_{G-REF} raise up to twelve. Table 9 presents the corresponding results.

Comparing tables 8-9 it is evident that the evaluation metrics rate drops significantly when the number of reference samples increases. Following and for the sake of simplicity, table 10 shows comparative results by means of the $EER_{user-threshold}^S$ only for the case in which each input signature was thinned not by the MOTL value of the claimed writer's reference set but with an OTL number provided for each individual signature. Clearly, the results that arise from the use of the MOTL value are inferior, an outcome that emphasizes the importance of the proposed preprocessing technique.

Table 11 demonstrates the influence of the segmentation profile to the verification performance in the case of the CEDAR dataset. Specifically, the following five segmentation scenarios were examined a) using the entire image (EI), b) applying the SP segmentation, c) using only the BRISK keypoints, d) EI in conjunction with SP and finally e) a conjunction of EI, SP and BRISK keypoints. It is evident that the proposed segmentation approach that uses EI, SP and BRISK keypoints outperforms all the other scenarios for all

TABLE 10
Indication of the influence ($EER\%$) imposed to the Verification performance among various cases of using:
I. MOTL and
II. Individual OTL values during the preprocessing stage.

F(A)	CEDAR		MCYT		GPD3300		UTSIG	
	MOTL	Ind.OTL	MOTL	Ind.OTL	MOTL	Ind.OTL	MOTL	Ind.OTL
F1	2.67	3.45	3.19	4.89	2.47	6.23	7.33	12.5
F2	4.17	5.20	8.65	10.2	3.98	8.65	11.4	24.9
F3	1.44	2.89	2.82	4.98	1.50	5.71	6.22	10.3
F4	7.51	9.42	16.7	20.5	15.2	20.5	20.1	26.0
F5	3.08	5.23	3.46	5.43	3.30	7.23	7.44	13.5

The EER^S rate corresponds to the user specific threshold case.

TABLE 11

Indication of the influence (EER %) imposed to the Verification performance among the cases of using different Segmentation profiles for the CEDAR signature dataset with l_0 -norm (KSVD/OMP).

Pooling Function F(A)	SP : $\beta = 2$ (Dim=360)				SP : $\beta = 3$ (Dim=660)			
	P_{FAR}^S	P_{FRR}	EER ^S	$P_{FAR}^{R \oplus EER^S}$	P_{FAR}^S	P_{FRR}	EER ^S	$P_{FAR}^{R \oplus EER^S}$
F1	13.6	13.5	8.13	0.53	12.1	9.37	7.33	0.25
F2	19.9	18.1	12.0	3.66	18.9	12.3	11.4	0.87
F3	13.2	11.5	7.36	0.33	9.77	8.17	6.22	0.12
F4	23.8	24.6	17.3	3.32	29.3	21.1	20.1	6.63
F5	13.9	12.7	8.51	0.39	10.1	9.55	7.44	0.21

Number of reference training samples $N_{G-REF} = 5$. The EER^S rate corresponds to the user specific threshold case.

pooling functions (with a minor exception of F5). Moreover, F3 feature vector persistently provided the best results in all segmentation scenarios and achieves the overall lower error in the proposed segmentation approach (last column of Table 11).

Perhaps the most challenging task on SV is the comparison of the results emanating from several state-of-the-art systems, as there is an abundance of degrees of freedom regarding the type or number of signatures utilized during the classifier construction and evaluation [51]. Still, Table 12 provides evidence that the proposed method achieves a low error of verification when a few genuine samples are available which is at least comparable to the ones derived from other state-of-the-art methods. It outlines and compares the $EER_{User_Threshold}^S$ based results of our proposed method, with emphasis to the F3 pooling, with a number of state-of-the-art SV related methods for the four utilized datasets on an EER or the average error AER basis.

VII. CONCLUSIONS

In this paper the potential of Sparse Representation on creating discriminative features for accurate and efficient offline signature verification was presented. We thoroughly investigated the major aspects on the selection of the appropriate SR approach, and examined the effects of the associated parameters. We demonstrated that approximate greedy techniques can deploy the full potential of SR in a SV system, in a computationally attractive manner. Further experiments revealed that non-negative constraints imposed in the SR optimization problem do not offer any advantage in terms of the overall system's discriminative ability. We described a novel pooling scheme tailored to the problem of SV, and evinced that 2nd order statistics can form more discriminative pooling functions in cases where signals exhibit degenerate structures. Finally, we proposed a carefully designed system, encompassing a novel algorithm for the automatic selection of the optimal thinning level, which is able to harness the power of SR in order to create a discriminative signature descriptor. The obtained state-of-the-art results on the most challenging signature datasets provide a strong indication towards the benefits of learned features, even in WD scenarios with only a few available reference samples. Our immediate future research plans includes among others the exploitation of SR related techniques in order to construct

TABLE 12

Listing of some Literature SV state-of-the-art techniques, results and comparisons with the proposed system.

1 st author / Ref #	Dataset	Method	# Samples	EER or AER
Kumar[58]	CEDAR	Signature Morphology	24[24] or 1[65]	11.6 / 11.8
Kumar[40]		Surroundness	24[24] or 1[65]	8.33
Chen[92]		Gradient & concavity	16	7.90
Chen[92]		Zemike moments	16	16.4
Kalera[89]		G. S & C	16	21.9
Guerba[46]		Curvelet Transform	12	5.60
Serdouk[29]		Gradient LBP + LRF	16	3.52
Hafemar[65]		SigNet	12	4.63
Bharathi[93]		Chain code	12	7.84
Okawa[22]		B.O.W with KAZE	16	1.60
Okawa[21]		V.L.A.D with KAZE	16	1.00
Ganapathi[94]		Gradient Direction	14	6.01
Shekar[95]		Morph Patt Spectrum	16	9.58
Hamaden[47]		Directional Co occurrence	5	2.11
Zois[17]		Archetypes	5	2.07
Dutta[23]		Compact Correlated Features	-	0.00
Zois[18]		Partially Ordered Sets	5	4.12
Proposed		KSVD/OMP (F3)	5	1.44
Vargas[36]	MCYT75	L.B.P	10	7.08
Zois[18]		Partially Ordered Sets	5	6.02
Gilperez[96]		Contours	10	7.08
Alonso- Fernandez[97]		Slant and envelope	5	22.4
Fierrez- Aguilar[52]		Global and local slant	10	9.28
Wen[59]		Invariant ring peripheral	5	15.0
Yin Ooi[53]		Discrete Radon transform	10	9.87
Soleiman[19]		HOG- Deep multitask metric	10	9.86
Hafemar[65]		SigNet	10	2.87
Serdouk[24]		H.O.T	10	18.2
Proposed		KSVD/OMP (F3)	5	2.82
Hu[98]	GPDS 150	LBP & HOG & GLCM	10	7.66
Yilmaz[45]	GPDS 160	LBP & HOG	12	6.97
Hafemar[65]		SigNet-F	5	2.41
Hafemar[65]		SigNet-F	12	1.72
Batista[68]		EoCs	12	16.8
Eskander[28]		ESC and DPDF codes	12	22.7
Alaei[49]	GPDS 300	LBP- based features	12	11.7
Pirlo[99]		Cosine similarity	12	7.20
Pirlo[37]		Optical flow	6	4.00
Parodi[56]		Circular Grid	13	4.21
Kumar[40]		Surroundness	24	13.8
Zois[18]		Partially Ordered Sets	5	5.48
Hafemar[65]		SigNet-F	5	2.42
Dutta[23]		Compact Correlated Features	-	11.2
Hafemar[65]		SigNet-F	12	1.69
Proposed		KSVD/OMP (F3)	5	1.50
Soleiman[19]	UTSIG	HOG- Deep multitask metric	12	17.6
Soleiman[91]		Fixed- point arithmetic,	12	29.7
Proposed		KSVD/OMP (F3)	12	6.22

a universal dictionary with the use of samples originating from a wider and diverse set of persons and not just only from one signatory in order to design a writer independent signature verifier.

REFERENCES

- [1] H.-L. Teulings, *Handwriting Movement Control*. London: Academic Press, 1996.
- [2] L. C. Alewijnse, "Analysis of Signature Complexity, Master Thesis," Master Thesis, University of Amsterdam, 2008.
- [3] G. Pirlo, M. Diaz, M. A. Ferrer, D. Impedovo, F. Occhionero, and U. Zurlo, "Early Diagnosis of Neurodegenerative Diseases by Handwritten Signature Analysis," *Cham*, pp. 290-297, 2015.
- [4] L. G. Hafemann, R. Sabourin, and L. S. Oliveira, "Offline Handwritten Signature Verification - Literature Review.," presented at the 7th International Conference on Image Processing Theory, Tools and Applications (IPTA 2017), Montreal, Canada, 2017.
- [5] D. Impedovo, G. Pirlo, and R. Plamondon, "Handwritten Signature Verification: New Advancements and Open Issues," presented at the 2012 International Conference on Frontiers in Handwriting Recognition, 2012.
- [6] R. Plamondon, G. Pirlo, and D. Impedovo, "Online Signature Verification," in *Handbook of Document Image Processing and Recognition*, D. Doermann and K. Tombre, Eds., ed London: Springer London, pp. 917-947, 2014.
- [7] S. Pal, M. Blumenstein, and U. Pal, "Off-line signature verification systems: a survey," presented at the Proceedings of the International Conference; Workshop on Emerging Trends in Technology, Mumbai, Maharashtra, India, 2011.
- [8] D. Impedovo and G. Pirlo, "Automatic Signature Verification: The State of the Art," *IEEE Transactions on Systems, Man and Cybernetics, Part C: Applications and Reviews*, vol. 38, pp. 609-635, 2008.
- [9] L. C. Alewijnse, C.E. van den Heuvel, and R. D. Stoel, "Analysis of signature complexity," *Journal of Forensic Document Examination*, vol. 21, pp. 37-49, 2011.
- [10] J. Wen, B. Fang, L. Zhang, and Y. Zhu, "Off-line Signature Verification Based on Multi-scale Local Structural Pattern," *International Journal of Pattern Recognition and Artificial Intelligence*, vol. 31, pp. 1756010-1 1756010-16, 2017.
- [11] J. Galbally, M. Diaz-Cabrera, M. A. Ferrer, M. Gomez-Barrero, A. Morales, and J. Fierrez, "On-line signature recognition through the combination of real dynamic data and synthetically generated static data," *Pattern Recognition*, vol. 48, pp. 2921-2934, 2015.
- [12] M. I. Malik, M. Liwicki, and A. Dengel, "Local features for off-line forensic signature verification " in *Advances in Digital Handwritten Signature Processing*, ed: World Scientific, pp. 95-109, 2014.
- [13] M. I. Malik, M. Liwicki, A. Dengel, S. Uchida, and V. Frinken, "Automatic Signature Stability Analysis and Verification Using Local Features," presented at the Proceedings 14th International Conference on Frontiers in Handwriting Recognition, 2014.
- [14] M. I. Malik and M. Liwicki, "From Terminology to Evaluation: Performance Assessment of Automatic Signature Verification Systems," presented at the 2012 International Conference on Frontiers in Handwriting Recognition, 2012.
- [15] R. A. Huber and A. M. Headrick, *Handwriting identification: facts and fundamentals*. Boca Raton: CRC Press, 2010.
- [16] E. N. Zois, I. Theodorakopoulos, D. Tsourounis, and G. Economou, "Parsimonious Coding and Verification of Offline Handwritten Signatures," presented at the 2017 IEEE Conference on Computer Vision and Pattern Recognition Workshops (CVPRW), 2017.
- [17] E. N. Zois, I. Theodorakopoulos, and G. Economou, "Offline Handwritten Signature Modeling and Verification Based on Archetypal Analysis," presented at the 2017 IEEE International Conference on Computer Vision (ICCV), 2017.
- [18] E. N. Zois, L. Alewijnse, and G. Economou, "Offline signature verification and quality characterization using poset-oriented grid features," *Pattern Recognition*, vol. 54, pp. 162-177, 2016.
- [19] A. Soleimani, B. N. Araabi, and K. Fouladi, "Deep Multitask Metric Learning for Offline Signature Verification," *Pattern Recognition Letters*, vol. 80, pp. 84-90, 2016.
- [20] S. Dey, A. Dutta, J. I. Toledo, S. K. Ghosh, J. Lladós, and U. Pal, "SigNet: Convolutional Siamese Network for Writer Independent Offline Signature Verification," *arXiv preprint arXiv:1707.02131*, 2017.
- [21] M. Okawa, "Vector of locally aggregated descriptors with KAZE features for offline signature verification," presented at the 2016 IEEE 5th Global Conference on Consumer Electronics, 2016.
- [22] M. Okawa, "Offline Signature Verification Based on Bag-Of-Visual Words Model Using KAZE Features and Weighting Schemes.," presented at the Proceedings of the IEEE Conference on Computer Vision and Pattern Recognition (CVPR) Workshops., 2016.
- [23] A. Dutta, U. Pal, and J. Lladós, "Compact correlated features for writer independent signature verification," presented at the 2016 23rd International Conference on Pattern Recognition (ICPR), 2016.
- [24] Y. Serdouk, H. Nemmour, and Y. Chibani, "Handwritten signature verification using the quad-tree histogram of templates and a Support Vector-based artificial immune classification," *Image and Vision Computing*, vol. 66, pp. 26-35, 2017.
- [25] B. A. Olshausen and D. J. Field, "Emergence of Simple-Cell Receptive-Field Properties by Learning a Sparse Code for Natural Images," *Nature*, vol. 381, pp. 607-609, 1996.
- [26] Z. Zhang, Y. Xu, J. Yang, X. Li, and D. Zhang, "A Survey of Sparse Representation: Algorithms and Applications," *IEEE Access*, vol. 3, pp. 490-530, 2015.

- [27] D. Rivard, E. Granger, and R. Sabourin, "Multi-feature extraction and selection in writer-independent off-line signature verification," *International Journal on Document Analysis and Recognition*, vol. 16, pp. 83-103, 2013.
- [28] G. S. Eskander, R. Sabourin, and E. Granger, "Hybrid writer-independent writer-dependent offline signature verification system," *IET Biometrics*, vol. 2, pp. 169-181, 2013.
- [29] Y. Serdouk, H. Nemmour, and Y. Chibani, "New off-line Handwritten Signature Verification method based on Artificial Immune Recognition System," *Expert Systems with Applications*, vol. 51, pp. 186-194, 2016.
- [30] Y. Serdouk, H. Nemmour, and Y. Chibani, "An improved Artificial Immune Recognition System for off-line handwritten signature verification," in *13th International Conference on Document Analysis and Recognition (ICDAR)*, pp. 196-200, 2015.
- [31] J. Coetzer, B. M. Herbst, and J. A. d. Preez, "Offline Signature Verification Using the Discrete Radon Transform and a Hidden Markov Model," *EURASIP Journal on Advances in Signal Processing*, vol. 2004, pp. 1-13, 2004.
- [32] E. J. R. Justino, F. Bortolozzi, and R. Sabourin, "A comparison of SVM and HMM classifiers in the off-line signature verification," *Pattern Recognition Letters*, vol. 26, pp. 1377-1385, 2005.
- [33] M. A. Ferrer, J. B. Alonso, and C. M. Travieso, "Offline geometric parameters for automatic signature verification using fixed-point arithmetic," *IEEE Transactions on Pattern Analysis and Machine Intelligence*, vol. 27, pp. 993-997, 2005.
- [34] H. Baltzakis and N. Papamarkos, "A new signature verification technique based on a two-stage neural network classifier," *Engineering Applications of Artificial Intelligence*, vol. 14, pp. 95-103, 2001.
- [35] F. Bin and T. Yuan Yan, "Improved class statistics estimation for sparse data problems in offline signature verification," *IEEE Transactions on Systems, Man, and Cybernetics, Part C (Applications and Reviews)*, vol. 35, pp. 276-286, 2005.
- [36] J. F. Vargas, M. A. Ferrer, C. M. Travieso, and J. B. Alonso, "Off-line signature verification based on grey level information using texture features," *Pattern Recognition*, vol. 44, pp. 375-385, 2011.
- [37] G. Pirlo and D. Impedovo, "Verification of Static Signatures by Optical Flow Analysis," *IEEE Transactions on Human-Machine Systems*, vol. 43, pp. 499-505, 2013.
- [38] L. G. Hafemann, R. Sabourin, and L. S. Oliveira, "Writer-independent feature learning for Offline Signature Verification using Deep Convolutional Neural Networks," presented at the 2016 International Joint Conference on Neural Networks (IJCNN), 2016.
- [39] D. Bertolini, L. S. Oliveira, E. Justino, and R. Sabourin, "Reducing forgeries in writer-independent off-line signature verification through ensemble of classifiers," *Pattern Recognition*, vol. 43, pp. 387-396, 2010.
- [40] R. Kumar, J. D. Sharma, and B. Chanda, "Writer-independent off-line signature verification using surroundedness feature," *Pattern Recognition Letters*, vol. 33, pp. 301-308, 2012.
- [41] M. A. Ferrer, M. Diaz-Cabrera, and A. Morales, "Static Signature Synthesis: A Neuromotor Inspired Approach for Biometrics," *Pattern Analysis and Machine Intelligence, IEEE Transactions on*, vol. 37, pp. 667-680, 2015.
- [42] M. Diaz, M. A. Ferrer, G. S. Eskander, and R. Sabourin, "Generation of Duplicated Off-Line Signature Images for Verification Systems," *IEEE Transactions on Pattern Analysis and Machine Intelligence*, vol. 39, pp. 951-964, 2017.
- [43] R. Sabourin, G. Genest, and F. J. Preteux, "Off-line signature verification by local granulometric size distributions," *IEEE Transactions on Pattern Analysis and Machine Intelligence* vol. 19, pp. 976-988, 1997.
- [44] M. A. Ferrer, J. F. Vargas, A. Morales, and A. Ordonez, "Robustness of Offline Signature Verification Based on Gray Level Features," *Information Forensics and Security, IEEE Transactions on*, vol. 7, pp. 966-977, 2012.
- [45] M. B. Yilmaz and B. Yanikoğlu, "Score level fusion of classifiers in off-line signature verification," *Information Fusion*, vol. 32, Part B, pp. 109-119, 2016.
- [46] Y. Guerbai, Y. Chibani, and B. Hadjadji, "The effective use of the one-class SVM classifier for handwritten signature verification based on writer-independent parameters," *Pattern Recognition*, vol. 48, pp. 103-113, 2015.
- [47] A. Hamadene and Y. Chibani, "One-Class Writer-Independent Offline Signature Verification Using Feature Dissimilarity Thresholding," *IEEE Transactions on Information Forensics and Security*, vol. 11, pp. 1226-1238, 2016.
- [48] C. Subhash and M. Sushila, "Static Signature Verification Based on Texture Analysis Using Support Vector Machine," *International Journal of Multimedia Data Engineering and Management (IJMDEM)*, vol. 8, pp. 22-32, 2017.
- [49] A. Alaei, S. Pal, U. Pal, and M. Blumenstein, "An Efficient Signature Verification Method Based on an Interval Symbolic Representation and a Fuzzy Similarity Measure," *IEEE Transactions on Information Forensics and Security*, vol. 12, pp. 2360-2372, 2017.
- [50] S. Pal, S. Chanda, U. Pal, K. Franke, and M. Blumenstein, "Off-line signature verification using G-SURF," in *12th International Conference on Intelligent Systems Design and Applications*, pp. 586-591, 2012.
- [51] H. Loka, E. Zois, and G. Economou, "Long range correlation of preceded pixels relations and application to off-line signature verification," *IET Biometrics*, vol. 6, issue 2, pp. 70-78, 2015.

- [52] J. Fierrez-Aguilar, N. Alonso-Hermira, G. Moreno-Marquez, and J. Ortega-Garcia, "An Off-line Signature Verification System Based on Fusion of Local and Global Information," in *Biometric Authentication*. vol. 3087, D. Maltoni and A. K. Jain, Eds., ed: Springer Berlin Heidelberg, pp. 295-306, 2004.
- [53] S. Y. Ooi, A. B. J. Teoh, Y. H. Pang, and B. Y. Hiew, "Image-based handwritten signature verification using hybrid methods of discrete Radon transform, principal component analysis and probabilistic neural network," *Applied Soft Computing*, vol. 40, pp. 274-282, 2016.
- [54] V. Nguyen, Y. Kawazoe, T. Wakabayashi, U. Pal, and M. Blumenstein, "Performance Analysis of the Gradient Feature and the Modified Direction Feature for Off-line Signature Verification," in *Proceedings International Conference on Frontiers in Handwriting Recognition*, pp. 303-307, 2010.
- [55] M. Diaz, M. A. Ferrer, G. Pirlo, G. Giannico, P. Henriquez, and D. Impedovo, "Off-line signature stability by optical flow: Feasibility study of predicting the verifier performance," in *2015 International Carnahan Conference on Security Technology (ICCSST)*, pp. 341-345, 2015.
- [56] M. Parodi, J. C. Gomez, and A. Belaid, "A Circular Grid-Based Rotation Invariant Feature Extraction Approach for Off-line Signature Verification," in *Proceedings 11th International Conference on Document Analysis and Recognition*, pp. 1289-1293, 2011.
- [57] J. Ruiz-del-Solar, C. Devia, P. Loncomilla, and F. Concha, "Offline Signature Verification Using Local Interest Points and Descriptors," in *Progress in Pattern Recognition, Image Analysis and Applications*. vol. 5197, J. Ruiz-Shulcloper and W. Kropatsch, Eds., ed: Springer Berlin Heidelberg, pp. 22-29, 2008.
- [58] R. Kumar, L. Kundu, B. Chanda, and J. D. Sharma, "A writer-independent off-line signature verification system based on signature morphology," presented at the Proceedings of the First International Conference on Intelligent Interactive Technologies and Multimedia, Allahabad, India, 2010.
- [59] J. Wen, B. Fang, Y. Y. Tang, and T. Zhang, "Model-based signature verification with rotation invariant features," *Pattern Recognition*, vol. 42, pp. 1458-1466, 2009.
- [60] B. Ribeiro, I. Gonçalves, S. Santos, and A. Kovacec, "Deep Learning Networks for Off-Line Handwritten Signature Recognition," presented at the Proceedings of the 16th Iberoamerican Congress conference on Progress in Pattern Recognition, Image Analysis, Computer Vision, and Applications, CIARP-11 Berlin, Heidelberg, 2011.
- [61] Khalajzadeh Hurieh, M. Mansouri, and M. Teshnehlal, "Persian Signature Verification using Convolutional Neural Networks," *International Journal of Engineering Research and Technology (IJERT)*, vol. 1, pp. 7-12, 2012.
- [62] Z. Zhang, X. Liu, and Y. Cui, "Multi-phase Offline Signature Verification System Using Deep Convolutional Generative Adversarial Networks," in *2016 9th International Symposium on Computational Intelligence and Design (ISCID)*, pp. 103-107, 2016.
- [63] H. Rantzs, H. Yang, and C. Meinel, "Signature Embedding: Writer Independent Offline Signature Verification with Deep Metric Learning," presented at the International Symposium on Visual Computing, Cham, 2016.
- [64] L. G. Hafemann, R. Sabourin, and L. S. Oliveira, "Analyzing features learned for Offline Signature Verification using Deep CNNs," presented at the 2016 23rd International Conference on Pattern Recognition (ICPR), 2016.
- [65] L. G. Hafemann, R. Sabourin, and L. S. Oliveira, "Learning features for offline handwritten signature verification using deep convolutional neural networks," *Pattern Recognition*, vol. 70, pp. 163-176, 2017.
- [66] R. Kumar, B. Chanda, and J. D. Sharma, "A novel sparse model based forensic writer identification," *Pattern Recognition Letters*, vol. 35, pp. 105-112, 2014.
- [67] Y. Liu, Z. Yang, and L. Yang, "Online Signature Verification Based on DCT and Sparse Representation," *IEEE Transactions on Cybernetics*, vol. 45, pp. 2498-2511, 2015.
- [68] L. Batista, E. Granger, and R. Sabourin, "Dynamic selection of generative-discriminative ensembles for off-line signature verification," *Pattern Recognition*, vol. 45, pp. 1326-1340, 2012.
- [69] Ng Andrew and Yu Kai. (2010). *ECCV-2010 Tutorial: Feature Learning for Image Classification*, <http://ufldl.stanford.edu/eccv10-tutorial/>.
- [70] N. Otsu, "A Threshold Selection Method from Gray-Level Histograms," *IEEE Transactions on Systems, Man and Cybernetics*, vol. 9, pp. 62-66, 1979.
- [71] S. Leutenegger, M. Chli, and R. Y. Siegwart, "BRISK: Binary Robust invariant scalable keypoints," in *2011 International Conference on Computer Vision*, pp. 2548-2555, 2011.
- [72] J. Yang, L. Zhang, Y. Xu, and J.-y. Yang, "Beyond sparsity: The role of L1-optimizer in pattern classification," *Pattern Recognition*, vol. 45, pp. 1104-1118, 2012.
- [73] R. Tibshirani, "Regression Shrinkage and Selection via the Lasso," *Journal of the Royal Statistical Society. Series B (Methodological)*, vol. 58, pp. 267-288, 1996.
- [74] J. A. Tropp and A. C. Gilbert, "Signal Recovery From Random Measurements Via Orthogonal Matching Pursuit," *IEEE Transactions on Information Theory*, vol. 53, pp. 4655-4666, 2007.
- [75] R. Rubinstein, M. Zibulevsky, and M. Elad, "Efficient implementation of the K-SVD algorithm using batch orthogonal matching pursuit," *CS Technion*, vol. 40, pp. 1-15, 2008.

- [76] S. S. Chen, D. L. Donoho, and M. A. Saunders, "Atomic Decomposition by Basis Pursuit," *SIAM Review*, vol. 43, pp. 129-159, 2001.
- [77] B. Efron, T. Hastie, I. Johnstone, and R. Tibshirani, "Least angle regression," *Ann. Statist.*, vol. 32, pp. 407-499, 2004.
- [78] J. Mairal, F. Bach, J. Ponce, and G. Sapiro, "Online Learning for Matrix Factorization and Sparse Coding," *J. Mach. Learn. Res.*, vol. 11, pp. 19-60, 2010.
- [79] J. Wang, J. Yang, K. Yu, F. Lv, T. Huang, and Y. Gong, "Locality-constrained Linear Coding for image classification," in *2010 IEEE Computer Society Conference on Computer Vision and Pattern Recognition*, pp. 3360-3367, 2010.
- [80] R. Rubinstein, A. M. Bruckstein, and M. Elad, "Dictionaries for Sparse Representation Modeling," *Proceedings of the IEEE*, vol. 98, pp. 1045-1057, 2010.
- [81] M. Aharon, M. Elad, and A. Bruckstein, "K -SVD: An Algorithm for Designing Overcomplete Dictionaries for Sparse Representation," *IEEE Transactions on Signal Processing*, vol. 54, pp. 4311-4322, 2006.
- [82] D. L. Donoho, "For most large underdetermined systems of linear equations the minimal " *Communications on Pure and Applied Mathematics*, vol. 59, pp. 797-829, 2006.
- [83] D. L. Donoho, "Neighborly polytopes and sparse solution of underdetermined linear equations.," Department of Statistics, Stanford University, 2004.
- [84] J. C. Yunchao Zhang, Xiujie Huang¹, Yongtian Wang, "A Probabilistic Analysis of Sparse Coded Feature Pooling and Its Application for Image Retrieval," *PLoS ONE.*, vol. 10, pp. 1-18, 2015.
- [85] G. Peyré, "Manifold models for signals and images," *Computer Vision and Image Understanding*, vol. 113, pp. 249-260, 2009.
- [86] P. J. Bickel, Y. a. Ritov, and A. B. Tsybakov, "Simultaneous analysis of Lasso and Dantzig selector," *Ann. Statist.*, vol. 37, pp. 1705-1732, 2009.
- [87] J. Feng, B. Ni, Q. Tian, and S. Yan, "Geometric lp-norm feature pooling for image classification," presented at the CVPR 2011, 2011.
- [88] H. Jégou, F. Perronnin, M. Douze, J. Sánchez, P. Pérez, and C. Schmid, "Aggregating Local Image Descriptors into Compact Codes," *IEEE Transactions on Pattern Analysis and Machine Intelligence*, vol. 34, pp. 1704-1716, 2012.
- [89] M. K. Kalera, S. Srihari, and A. Xu, "Offline signature verification and identification using distance statistics," *International Journal of Pattern Recognition and Artificial Intelligence*, vol. 18, pp. 1339-1360, 2004.
- [90] J. Ortega-Garcia, J. Fierrez-Aguilar, D. Simon, J. Gonzalez, M. Faundez-Zanuy, V. Espinosa, *et al.*, "MCYT baseline corpus: a bimodal biometric database," *IEE Proceedings Vision, Image and Signal Processing*, vol. 150, pp. 395-401, 2003.
- [91] A. Soleimani, K. Fouladi, and B. N. Araabi, "UTSig: A Persian offline signature dataset," *IET Biometrics*, vol. 6, pp. 1-8, 2016.
- [92] S. Chen and S. Srihari, "A New Off-line Signature Verification Method based on Graph," presented at the Proceedings 18th International Conference on Pattern Recognition, 2006.
- [93] R. K. Bharathi and B. H. Shekar, "Off-line signature verification based on chain code histogram and Support Vector Machine," presented at the Advances in Computing, Communications and Informatics (ICACCI), 2013 International Conference on, 2013.
- [94] G. Ganapathi and R. Nadarajan, "A Fuzzy Hybrid Framework for Offline Signature Verification," in *Pattern Recognition and Machine Intelligence: 5th International Conference, PReMI 2013, Kolkata, India, December 10-14, 2013. Proceedings*, P. Maji, A. Ghosh, M. N. Murty, K. Ghosh, and S. K. Pal, Eds., ed Berlin, Heidelberg: Springer Berlin Heidelberg, pp. 121-127, 2013.
- [95] B. H. Shekar, R. K. Bharathi, and B. Pilar, "Local Morphological Pattern Spectrum Based Approach for Off-line Signature Verification," in *Pattern Recognition and Machine Intelligence: 5th International Conference, PReMI 2013, Kolkata, India, December 10-14, 2013. Proceedings*, P. Maji, A. Ghosh, M. N. Murty, K. Ghosh, and S. K. Pal, Eds., ed Berlin, Heidelberg: Springer Berlin Heidelberg, pp. 335-342, 2013.
- [96] A. Gilperez, F. Alonso-Fernandez, S. Pecharroman, J. Fierrez, and J. Ortega-Garcia, "Off-line Signature Verification Using Contour Features," presented at the Proceedings 11th International Conference on Frontiers in Handwriting Recognition, Montreal, 2008.
- [97] F. Alonso-Fernandez, M. C. Fairhurst, J. Fierrez, and J. Ortega-Garcia, "Automatic Measures for Predicting Performance in Off-Line Signature," presented at the IEEE International Conference on Image Processing, 2007.
- [98] J. Hu and Y. Chen, "Offline Signature Verification Using Real Adaboost Classifier Combination of Pseudo-dynamic Features," in *12th International Conference on Document Analysis and Recognition*, pp. 1345-1349, 2013.
- [99] G. Pirlo and D. Impedovo, "Cosine similarity for analysis and verification of static signatures," *IET Biometrics*, vol. 2, pp. 151-158, 2013.